Search for B decays into $\eta' p$, $\eta' K^*$, $\eta' \phi$, $\eta' \omega$ and $\eta' \eta^{(\prime)}$

J. Schümann,[21] C. H. Wang,[21] K. Abe,[5] H. Aihara,[41] D. Anipko,[47] K. Arinstein,[47] V. Aulchenko,[47] T. Aushev,[9,14] A. M. Bakich,[36] E. Barberio,[17] K. Belous,[8] U. Bitenc,[10] I. Bizjak,[10] S. Blyth,[20] A. Bondar,[47] A. Bozek,[23] M. Bračko,[5,10,16] T. E. Browder,[4] P. Chang,[22] Y. Chao,[22] A. Chen,[20] K.-F. Chen,[22] W. T. Chen,[20] B. G. Cheon,[3] R. Chistov,[9] Y. Choi,[35] Y. K. Choi,[35] S. Cole,[36] J. Dalseno,[17] S. Eidelman,[47] S. Fratina,[10] T. Gershon,[5] A. Go,[20] G. Gokhroo,[37] B. Golob,[10,15] H. Ha,[12] M. Hazumi,[5] D. Heffernan,[28] T. Hokuue,[18] Y. Hoshi,[39] S. Hou,[20] W.-S. Hou,[22] Y. B. Hsiung,[22] K. Ikado,[18] A. Imoto,[19] K. Inami,[18] A. Ishikawa,[41] R. Itoh,[5] M. Iwasaki,[41] Y. Iwasaki,[5] J. H. Kang,[46] P. Kapusta,[23] N. Katayama,[5] H. Kawai,[48] T. Kawasaki,[25] H. R. Khan,[42] H. Kichimi,[5] H. O. Kim,[35] Y. J. Kim,[2] K. Kinoshita,[1] S. Korpar,[10,16] P. Križan,[10,15] P. Krokovny,[5] R. Kulasiri,[1] R. Kumar,[29] C. C. Kuo,[20] A. Kuzmin,[47] Y.-J. Kwon,[46] M. J. Lee,[33] S. E. Lee,[33] T. Lesiak,[23] A. Limosani,[5] S.-W. Lin,[22] D. Liventsev,[9] G. Majumder,[37] F. Mandl,[7] D. Marlow,[31] T. Matsumoto,[43] A. Matyja,[23] S. McOnie,[36] T. Medvedeva,[9] H. Miyata,[25] Y. Miyazaki,[18] R. Mizuk,[9] T. Mori,[18] Y. Nagasaka,[6] E. Nakano,[27] M. Nakao,[5] H. Nakazawa,[5] S. Nishida,[5] O. Nitoh,[44] S. Ogawa,[38] T. Ohshima,[18] S. Okuno,[11] Y. Onuki,[32] H. Ozaki,[5] P. Pakhlov,[9] G. Pakhlova,[9] C. W. Park,[35] H. Park,[13] K. S. Park,[35] L. S. Peak,[36] R. Pestotnik,[10] L. E. Piilonen,[45] Y. Sakai,[5] N. Satoyama,[34] T. Schietinger,[14] O. Schneider,[14] C. Schwanda,[7] K. Senyo,[18] M. E. Sevior,[17] M. Shapkin,[8] H. Shibuya,[38] A. Somov,[1] S. Stanič,[26] M. Starič,[10] H. Stoeck,[36] S. Y. Suzuki,[5] F. Takasaki,[5] K. Tamai,[5] M. Tanaka,[5] G. N. Taylor,[17] Y. Teramoto,[27] X. C. Tian,[30] I. Tikhomirov,[9] K. Trabelsi,[5] T. Tsuboyama,[5] T. Tsukamoto,[5] S. Uehara,[5] T. Uglov,[9] K. Ueno,[22] S. Uno,[5] P. Urquijo,[17] Y. Usov,[47] G. Varner,[4] S. Villa,[14] M.-Z. Wang,[22] M. Watanabe,[25] Y. Watanabe,[42] E. Won,[12] A. Yamaguchi,[40] Y. Yamashita,[24] M. Yamauchi,[5] V. Zhilich,[47] and A. Zupanc[10]

(Belle Collaboration)

[1]*University of Cincinnati, Cincinnati, Ohio 45221*
[2]*The Graduate University for Advanced Studies, Hayama*
[3]*Hanyang University, Seoul*
[4]*University of Hawaii, Honolulu, Hawaii 96822*
[5]*High Energy Accelerator Research Organization (KEK), Tsukuba*
[6]*Hiroshima Institute of Technology, Hiroshima*
[7]*Institute of High Energy Physics, Vienna*
[8]*Institute of High Energy Physics, Protvino*
[9]*Institute for Theoretical and Experimental Physics, Moscow*
[10]*J. Stefan Institute, Ljubljana*
[11]*Kanagawa University, Yokohama*
[12]*Korea University, Seoul*
[13]*Kyungpook National University, Taegu*
[14]*Swiss Federal Institute of Technology of Lausanne, EPFL, Lausanne*
[15]*University of Ljubljana, Ljubljana*
[16]*University of Maribor, Maribor*
[17]*University of Melbourne, Victoria*
[18]*Nagoya University, Nagoya*
[19]*Nara Women's University, Nara*
[20]*National Central University, Chung-li*
[21]*National United University, Miao Li*
[22]*Department of Physics, National Taiwan University, Taipei*
[23]*H. Niewodniczanski Institute of Nuclear Physics, Krakow*
[24]*Nippon Dental University, Niigata*
[25]*Niigata University, Niigata*
[26]*University of Nova Gorica, Nova Gorica*
[27]*Osaka City University, Osaka*
[28]*Osaka University, Osaka*
[29]*Panjab University, Chandigarh*
[30]*Peking University, Beijing*
[31]*Princeton University, Princeton, New Jersey 08544*
[32]*RIKEN BNL Research Center, Upton, New York 11973*
[33]*Seoul National University, Seoul*
[34]*Shinshu University, Nagano*
[35]*Sungkyunkwan University, Suwon*

[36]*University of Sydney, Sydney New South Wales*
[37]*Tata Institute of Fundamental Research, Bombay*
[38]*Toho University, Funabashi*
[39]*Tohoku Gakuin University, Tagajo*
[40]*Tohoku University, Sendai*
[41]*Department of Physics, University of Tokyo, Tokyo*
[42]*Tokyo Institute of Technology, Tokyo*
[43]*Tokyo Metropolitan University, Tokyo*
[44]*Tokyo University of Agriculture and Technology, Tokyo*
[45]*Virginia Polytechnic Institute and State University, Blacksburg, Virginia 24061*
[46]*Yonsei University, Seoul*
[47]*Budker Institute of Nuclear Physics, Novosibirsk*
[48]*Chiba University, Chiba*
(Received 26 January 2007; published 15 May 2007)

We report on a search for the exclusive two-body charmless hadronic B meson decays $B \to \eta' \rho$, $B \to \eta' K^*$, $B^0 \to \eta' \phi$, $B^0 \to \eta' \omega$, and $B^0 \to \eta' \eta^{(\prime)}$. The results are obtained from a data sample containing 535×10^6 $B\bar{B}$ pairs that were collected at the $\Upsilon(4S)$ resonance with the Belle detector at the KEKB asymmetric-energy e^+e^- collider. We find no significant signals and report upper limits in the range $(0.5\text{–}6.5) \times 10^{-6}$ for all of the above decays.

DOI: 10.1103/PhysRevD.75.092002 PACS numbers: 13.25.Hw, 11.30.Er

I. INTRODUCTION

Information on the two-body charmless hadronic B meson decays with an η' meson in the final state ($B \to \eta' h^{(*)}$) is incomplete at the present. While the decay $B \to \eta' K$ is observed with a large branching fraction, so far no other $B \to \eta' h^{(*)}$ decay mode has been observed with greater than 5σ significance. The first evidence of $B \to \eta' \pi$ has recently been reported [1,2] and *BABAR* found evidence for $B \to \eta' K^*$ with larger than 4σ significance [3], and thus additional observations are expected in the near future. The study of these decay modes can improve the understanding of the flavor-singlet penguin amplitude with intermediate t, c, and u quarks [4]. Furthermore, these studies increase our confidence in the reliability of a variety of other predictions, e.g., for the CP violating parameter ϕ_3 (γ), and are necessary to extract theory parameters such as the scalar penguin operator [4,5]. Presently, theoretical predictions for the branching fractions of these decay modes cover the range $(0.0001\text{–}7.6) \times 10^{-6}$ [4–6]. The most stringent upper limits for presently unobserved decays were reported by *BABAR* [1,3,7].

II. DATA SET AND APPARATUS

The study performed here includes the decays $B^{(0,+)} \to \eta' \rho^{(0,+)}$, $B^{(0,+)} \to \eta' K^{*(0,+)}$, $B^0 \to \eta' \phi$, $B^0 \to \eta' \omega$, and $B^0 \to \eta' \eta^{(\prime)}$ and is based on a data sample that contains 535×10^6 $B\bar{B}$ pairs, collected with the Belle detector at the KEKB asymmetric energy e^+e^- (3.5 GeV on 8 GeV) collider [8]. Throughout this paper, the inclusion of the charge conjugate decay is implied unless stated otherwise.

KEKB operates at the $\Upsilon(4S)$ resonance ($\sqrt{s} = 10.58$ GeV) with a peak luminosity that exceeds 1.7×10^{34} cm^{-2} s^{-1}. The Belle detector is a large-solid-angle magnetic spectrometer that consists of a silicon vertex detector (SVD), a 50-layer central drift chamber (CDC), an array of aerogel threshold Čherenkov counters (ACC), a barrel-like arrangement of time-of-flight scintillation counters (TOF), and an electromagnetic calorimeter comprised of CsI(Tl) crystals located inside a superconducting solenoid coil that provides a 1.5 T magnetic field. An iron flux-return located outside of the coil is instrumented to detect K_L^0 mesons and to identify muons. The detector is described in detail elsewhere [9]. Two inner detector configurations were used. A 2.0 cm beampipe and a 3-layer SVD were used for the first data sample of 152×10^6 $B\bar{B}$ pairs (Set *I*), while a 1.5 cm beampipe, a 4-layer SVD, and a small-cell inner drift chamber were used to record the remaining 383×10^6 $B\bar{B}$ pairs (Set *II*) [10].

III. EVENT SELECTION AND RECONSTRUCTION

For what follows, unless stated otherwise, all variables are defined in the center-of-mass frame with the z axis antiparallel to the positron direction.

Charged hadrons are identified by combining information from the CDC (dE/dx), ACC, and TOF systems. Both kaons and pions are selected with an average efficiency of 86% and are misidentified as pions or kaons, respectively, in 4% of the cases.

The η' mesons are reconstructed in the decays $\eta' \to \eta\pi^+\pi^-$ (with $\eta \to \gamma\gamma$) and $\eta' \to \rho^0\gamma$, except for the decays $B^0 \to \eta'\eta$, $B^0 \to \eta'\eta'$, and $B^0 \to \eta'\omega$, which use only the $\eta' \to \eta\pi^+\pi^-$ channel. We define the η' ($h^{(*)}$) side as all particles involved in the decay of the η' ($h^{(*)}$) from the decay $B \to \eta' h^{(*)}$. The η, ρ^0, and η' candidates on the η' side are reconstructed using the mass windows given in Table I. Mass windows used to reconstruct the $h^{(*)}$ are given in Table II. In addition, we require the following:

TABLE I. Invariant mass windows used to select intermediate states on the η' side. σ denotes a standard deviation of the reconstructed mass distribution.

Mode	Mass window (MeV/c^2)	Mass window in units of σ
$\rho^0 \to \pi^+\pi^-$	[550, 870]	—
$\eta \to \gamma\gamma$	[500, 570]	$+2.5/-3.3$
$\eta' \to \eta\pi^+\pi^-$	[950, 965]	± 2.5
$\eta' \to \rho^0\gamma$	[941, 970]	± 2.5

photons originating from π^0 and η decays are required to have energies of at least 100 MeV, photons from the η' in $\eta' \to \rho^0\gamma$ have to be above 200 MeV in the laboratory frame. The transverse momenta of the $\pi^\pm$ for $\eta' \to \eta_{\gamma\gamma}\pi^+\pi^-$ ($\eta' \to \rho^0_{\pi^+\pi^-}\gamma$) candidates have to be greater than 100 MeV/c (200 MeV/c). An additional requirement on the cosine of the ρ^0 helicity angle in $\eta' \to \rho^0\gamma$ of $|\cos\theta_h| < 0.85$ is applied, where θ_h is the angle between the momenta of one of the daughter pions of the ρ^0 and the η' in the ρ^0 rest frame. The vertex of the $K^0_S \to \pi^+\pi^-$ has to be displaced from the interaction point (IP) and the K^0_S momentum direction must be consistent with its flight direction as indicated in Table III [11].

B meson candidates are formed by combining an η' meson with one of the hadrons listed in Table II excluding π^0's and K^0_S's. B candidates are identified using two kinematic variables: the energy difference, $\Delta E = E_B - E_{\mathrm{beam}}$, and the beam-energy constrained mass, $M_{\mathrm{bc}} = \sqrt{E_{\mathrm{beam}}/c^4 - (P_B/c)^2}2$, where E_{beam} is the beam energy and E_B (P_B) is the reconstructed energy (momentum) of the B candidate. Signal events peak at $\Delta E = 0$ GeV and $M_{\mathrm{bc}} = M_B$, where M_B is the B meson mass, with resolutions around 15 MeV and 3 MeV for ΔE and M_{bc}, respectively. An η mass constraint fit is applied in the $\eta' \to \eta\pi^+\pi^-$ subdecay in order to improve the ΔE resolution. Here the two photons from $\eta \to \gamma\gamma$ are constrained to have the nominal η mass given by the Particle Data Group (PDG) [12]. Events satisfying the requirements $M_{\mathrm{bc}} > 5.22$ GeV$/c^2$ and $|\Delta E| < 0.25$ GeV are selected for further analysis. After all selections are applied, depending on the decay mode between 3% and 20% of the events have multiple B candidates in one event. A χ^2 variable is calculated to select the best candidate of such events. We select the B with the smallest $\chi^2 = \chi^2_{\mathrm{vtx}} + \chi^2(M_{\eta'}) + \chi^2(M_{h^{(*)}})$, where χ^2_{vtx} is an estimator of the vertex quality for all charged particles not from the K^0_S and $\chi^2(M_X) = [(M_X - m_X)/\sigma_X]^2$, where M_X (m_X) is the reconstructed (nominal) mass of the particle candidate $X(= \eta'$ or $h^{(*)})$ and σ_X is the standard deviation of the reconstructed X mass distribution as obtained from fits to MC distributions.

TABLE II. Invariant mass windows used to select intermediate states on the $h^{(*)}$ side. σ denotes a standard deviation of the reconstructed mass distribution.

Mode	Mass window (MeV/c^2)	Mass window in units of σ
$\pi^0 \to \gamma\gamma$	[118, 150]	± 2.5
$K^0_S \to \pi^+\pi^-$	[485, 510]	± 3
$\rho^+ \to \pi^+\pi^0$	[620, 920]	—
$\rho^0 \to \pi^+\pi^-$	[620, 920]	—
$K^{*0} \to K^+\pi^-$	[820, 965]	—
$K^{*+} \to K^0_S\pi^+$	[820, 965]	—
$K^{*+} \to K^+\pi^0$	[820, 965]	—
$\phi \to K^+K^-$	[1010, 1030]	± 3
$\eta \to \gamma\gamma$	[510, 575]	± 2.5
$\eta' \to \eta\pi^+\pi^-$	[950, 965]	± 2.5
$\omega \to \pi^+\pi^-\pi^0$	[750, 810]	± 2.5

TABLE III. Selection criteria for the distance of closest approach of one of the K^0_S daughter pions to the IP (dr) in the x-y plane, azimuthal angle between the momentum vector and the flight direction of the K^0_S candidate inferred from the production and decay vertexes ($d\phi$), distance of closest approach between the two daughter tracks (z-dist.), and the flight length of the K^0_S candidate in the x-y plane (fl).

Momentum (GeV/c)	dr (cm)	$d\phi$ (rad)	z-dist. (cm)	fl (cm)
<0.5	>0.05	<0.3	<0.8	—
0.5–1.5	>0.03	<0.1	<1.8	>0.08
>1.5	>0.02	<0.03	<2.4	>0.22

IV. BACKGROUND SUPPRESSION

The dominant background for this analysis is continuum $e^+e^- \to q\bar{q}$ ($q = u, d, s, c$). Other background sources are charmless B decays such as $B \to \eta' K$ and $b \to c$ decays. The background is 90% continuum with the remaining 10% nearly evenly split between the other two contributions.

Several event shape variables are used to distinguish the spherical $B\bar{B}$ topology from the jetlike $e^+e^- \to q\bar{q}$ continuum background. The thrust angle θ_T is defined as the angle between the η' momentum direction and the thrust axis formed by all particles not belonging to the reconstructed B meson. Continuum events tend to peak near $|\cos\theta_T| = 1$, while $B\bar{B}$ events have a uniform distribution. The requirement $|\cos\theta_T| < 0.9$ is applied prior to all other event topology selections resulting in a signal efficiency (background reduction) of 90% (56%).

Additional continuum background suppression is obtained by using modified Fox-Wolfram moments [13] and $|\cos\theta_B|$, where θ_B is the angle between the flight direction of the reconstructed B candidate and the beam axis. A Fisher discriminant ($\mathcal{F}$) [14] is formed from a linear combination of $|\cos\theta_T|$, $S_\perp$ [15] and five modified Fox-Wolfram moments. $S_\perp$ is the ratio of the scalar sum of the

transverse momenta of all tracks outside a 45° cone around the η' direction to the scalar sum of their total momenta. The Fisher discriminant is then combined with the B flight direction information to form an event topology likelihood function $\mathcal{L}_S$ ($\mathcal{L}_{q\bar{q}}$), where the subscript S ($q\bar{q}$) represents signal (continuum background). The signal over continuum background ratio varies over the range of the quality parameter r of the B flavor tagging of the accompanying B meson. We use the standard Belle B tagging algorithm [16], which gives the B flavor and the tagging quality r ranging from zero for no flavor to unity for unambiguous flavor assignment. The data is divided into three r regions and the likelihood ratio $\mathcal{R}_L = \mathcal{L}_S/(\mathcal{L}_S + \mathcal{L}_{q\bar{q}})$ requirements are determined to maximize $N_S/\sqrt{N_B}$, with N_S (N_B) the expected number of signal (background), on Monte Carlo (MC) events in each r region separately. More stringent selections are imposed for the first r region at zero while looser criteria are used for r close to 1. More stringent selections are applied for decays with large continuum contribution such as $B \to \eta'\rho$, while relatively clean decays such as $B^0 \to \eta'\phi$ have very loose requirements. The signal efficiencies (continuum background reduction) lie in the range of 42%–88% (98%–45%).

Contributions from other charmless B decays can contaminate the signal when a pion is misidentified as a kaon or when a random pion is added or missed. The dominant contribution for such misidentified events originates from $B \to \eta' K$ decays. For the decays $B \to \eta'\rho$, $B \to \eta' K^*$, and $B^0 \to \eta'\omega$ the $B \to \eta' K$ contamination is significant. For these decays we construct an alternative B meson hypothesis assuming that it originates from a $B \to \eta' K$ decay. We then veto an event if the alternative ΔE variable is within a decay-dependent window around $\Delta E = 0$ GeV and $M_{\rm bc} > 5.27$ GeV/c. The selection is optimized for each decay and results in negligible signal suppression ($< 0.5\%$) while removing around 80% of the $B \to \eta' K$ background.

V. MEASUREMENT OF BRANCHING FRACTIONS

The branching fractions are obtained using an extended unbinned maximum-likelihood fit to the ΔE and $M_{\rm bc}$ distributions of selected events. This fit is performed simultaneously in the $\eta' \to \eta\pi^+\pi^-$ and $\eta' \to \rho^0\gamma$ subdecay channels for all B decay modes, where applicable. In the case of $B^+ \to \eta' K^{*+}$ the two K^{*+} subdecay modes (thus four subdecay channels in total) are fitted simultaneously. The extended likelihood function used is:

$$L(N_S, N_{B_j}) = \frac{e^{-(N_S + \sum_j N_{B_j})}}{N!} \prod_{i=1}^{N} \Big[N_S P_S(\Delta E_i, M_{\rm bc_i}) + \sum_j N_{B_j} P_{B_j}(\Delta E_i, M_{\rm bc_i}) \Big], \quad (1)$$

where N_S (N_{B_j}) is the number of signal events (background events of source j) with probability density functions (PDFs) P_S (P_{B_j}). The index i runs from 1 to the total number of events N in the selected sample.

The branching fraction $\mathcal{B}$ is determined by maximizing the combined likelihood for both data sets and all subdecays with $\mathcal{B}$ constrained to be the same for the subdecays. The number of signal events (N_S) for each decay mode is calculated by $N_S = \mathcal{B}[N_{B\bar{B}}(I)\epsilon_{\rm t}(I) + N_{B\bar{B}}(II)\epsilon_{\rm t}(II)]$, where $N_{B\bar{B}}(k)$ is the number of $B\bar{B}$ produced for set $k = I$ or II and $\epsilon_{\rm t}(k)$ is the total reconstruction efficiency including subdecay branching fractions for set k.

The reconstruction efficiencies are determined from signal MC samples using the EvtGen package [17] with final state radiation simulated by the PHOTOS package [18] (thus measuring $B \to \eta' h^{(*)}(\gamma)$). The efficiencies are calculated separately for Set I and Set II. The absolute efficiency for Set II is typically about 0.5% larger than for Set I (for efficiencies averaged over the two sets see Tables IV and V). Corrections due to differences between data and MC are included for the charged track identification and photon, π^0, and η reconstructions, resulting in an overall correction factor between 0.88 and 0.99 depending on the decay mode. We assume the numbers of B^+B^- and $B^0\bar{B}^0$ pairs to be equal in the original data sample.

In the fit to the data we consider a signal component and three types of background components: continuum events,

TABLE IV. Average efficiencies (ϵ) for the two data sets for $\eta' \to \eta\pi^+\pi^-$ and $\eta' \to \rho^0\gamma$, total efficiencies ($\epsilon_{\rm t}$) with systematic errors of secondary branching fractions included, signal yield (N_S) with statistical errors only, and the 90% confidence level upper limit on the branching fraction in units of 10^{-6} including systematic errors for each decay of this analysis (UL) and latest results from *BABAR* in units of 10^{-6}.

	$B^0 \to \eta'\rho^0$	$B^+ \to \eta'\rho^+$	$B^0 \to \eta' K^{*0}$	$B^+ \to \eta' K^{*+}$	$B^0 \to \eta'\phi$
$\epsilon(\eta\pi\pi)$ [%]	7.0 ± 0.1	5.9 ± 0.1	8.5 ± 0.1	4.5 ± 0.1	12.9 ± 0.1
$\epsilon(\rho\gamma)$ [%]	5.4 ± 0.1	3.9 ± 0.1	5.9 ± 0.1	2.2 ± 0.1	7.4 ± 0.1
$\epsilon_{\rm t}(\eta\pi\pi)$ [%]	1.13 ± 0.02	0.93 ± 0.02	0.92 ± 0.01	0.35 ± 0.01	1.08 ± 0.01
$\epsilon_{\rm t}(\rho\gamma)$ [%]	1.51 ± 0.03	1.07 ± 0.02	1.09 ± 0.02	0.30 ± 0.01	1.08 ± 0.02
N_S [%]	$0.1^{+8.2}_{-7.0}$	$18.5^{+23.3}_{-21.7}$	$14.2^{+9.1}_{-8.0}$	$-6.4^{+10.9}_{-7.9}$	$-2.4^{+2.5}_{-3.5}$
UL [10^{-6}]	<1.3	<5.8	<2.6	<2.9	<0.5
BABAR [10^{-6}]	<3.7	<14	$3.8 \pm 1.1 \pm 0.5$	$4.9^{+1.9}_{-1.7} \pm 0.8$	<4.5

TABLE V. Average efficiencies (ϵ) for the two data sets for $\eta' \to \eta\pi^+\pi^-$, total efficiencies (ϵ_t) with systematic errors of secondary branching fractions included, signal yield (N_S) with statistical errors only and the 90% confidence level upper limit on the branching fraction in units of 10^{-6} including systematic errors for each decay of this analysis (UL), and latest results from *BABAR* in units of 10^{-6}.

	$B^0 \to \eta'\eta$	$B^0 \to \eta'\eta'$	$B^0 \to \eta'\omega$
$\epsilon(\eta\pi\pi)$ [%]	5.7 ± 0.1	4.8 ± 0.1	7.5 ± 0.1
$\epsilon_t(\eta\pi\pi)$ [%]	0.37 ± 0.007	0.16 ± 0.003	1.09 ± 0.02
N_S	$1.0^{+4.6}_{-3.6}$	$-6.3^{+2.2}_{-2.1}$	$0.9^{+6.3}_{-5.2}$
UL [10^{-6}]	<4.5	<6.5	<2.2
BABAR [10^{-6}]	<1.7	<10	<2.8

events from other B meson decays via the dominant $b \to c$ transition, and from charmless B decays.

For both signal and continuum background ΔE and M_{bc} are uncorrelated and we use two independent functions to describe the shapes of ΔE and M_{bc}. To model the signal, we use a Gaussian with an exponential tail, the so-called Crystal Ball-line (CBline) function [19], plus a Gaussian in ΔE, while M_{bc} is described by a single CBline function. The shape parameters are fixed from the signal MC study. Corrections for MC-data discrepancies determined from control samples of $B^+ \to \eta' K^+$ and $B^+ \to D^0\pi^0$, where $D^0 \to K^-\pi^+$ and $D^0 \to K^-\pi^+\pi^0$, are applied to the mean and width of the CBline functions.

Continuum background is modeled by a first-order polynomial for ΔE and an ARGUS function [20] for M_{bc}. The continuum shape parameters, that are allowed to float in all modes, are the slopes of the polynomial and ARGUS function. The shapes for charmless B decays remaining after applying the vetoes and $b \to c$ backgrounds are modeled by two-dimensional smoothed histograms. The sizes of background contributions other than the continuum background are fixed to the values expected from MC studies.

The resulting ΔE and M_{bc} projections are shown in Figs. 1 and 2. The reconstruction efficiencies and fit results are given in Tables IV and V.

VI. SYSTEMATICS

Systematic errors on the branching fractions are estimated with various high statistics data samples. The dominant sources are the uncertainties in the reconstruction efficiency of charged tracks (3%–4%), the uncertainties in the reconstruction efficiencies of η mesons, π^0's, and photons (3%–6%) and the K^0_S reconstruction efficiency uncertainty (4%). Other systematic uncertainties arise from signal MC statistics (2%), likelihood ratio selections

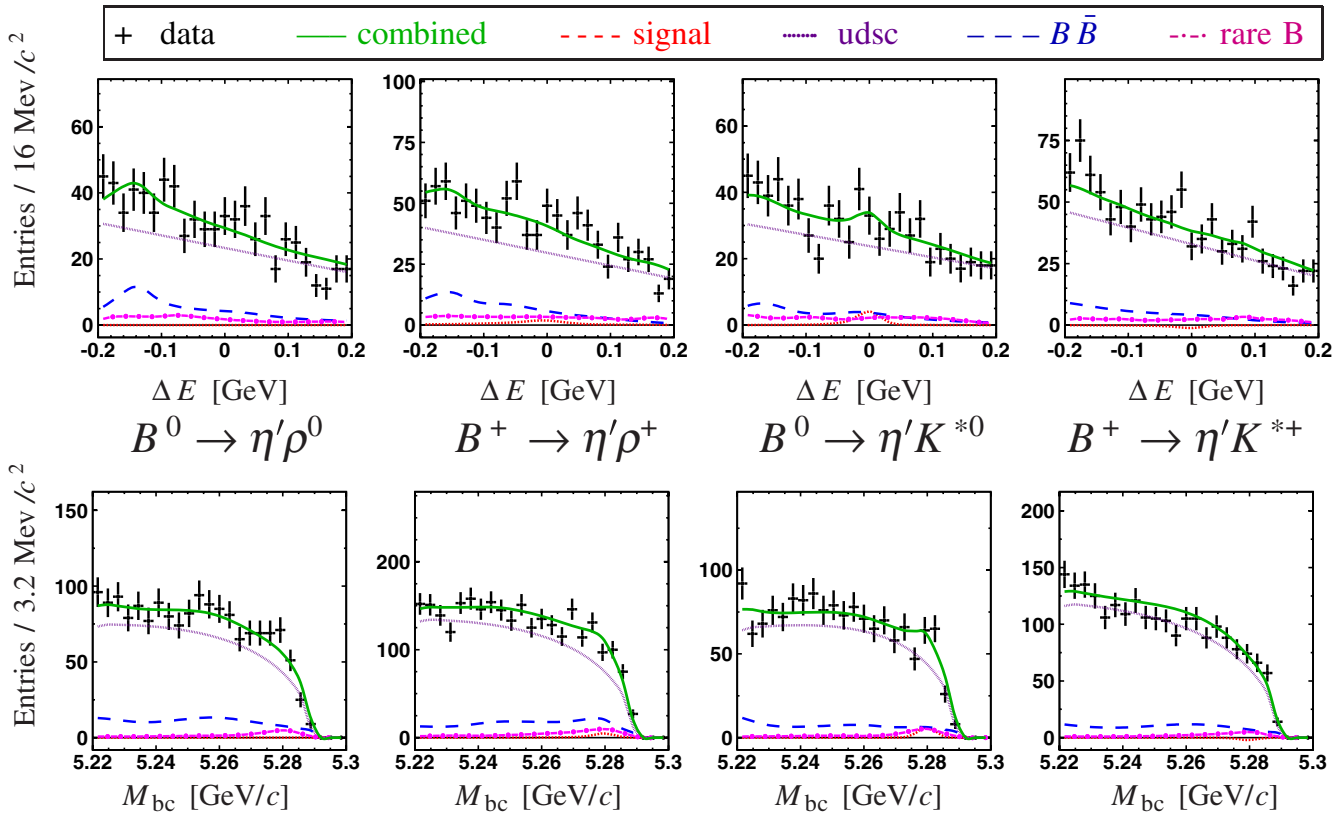

FIG. 1 (color online). ΔE (upper) and M_{bc} (lower) distributions for (from left to right) $B^0 \to \eta'\rho^0$, $B^+ \to \eta'\rho^+$, $B^0 \to \eta' K^{*0}$, and $B^+ \to \eta' K^{*+}$.

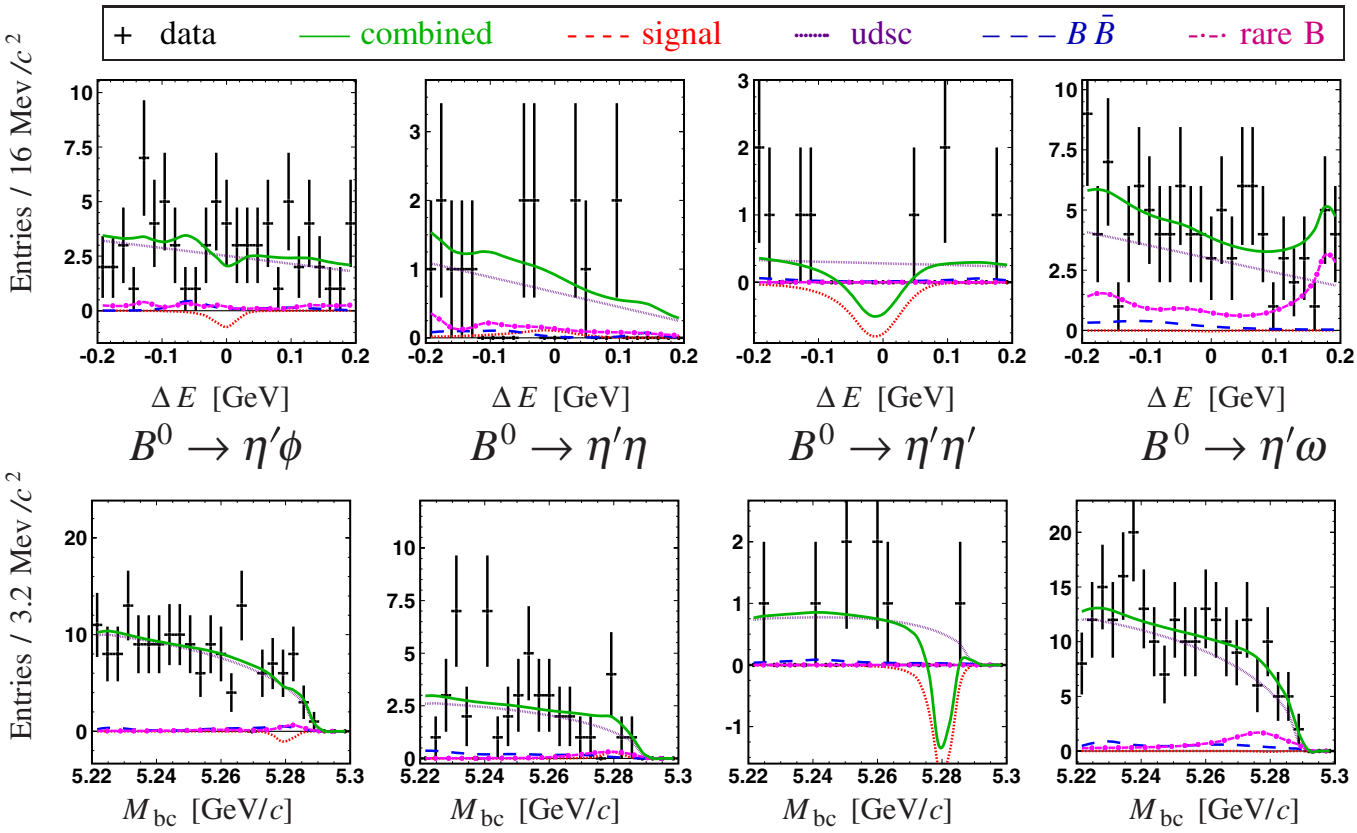

FIG. 2 (color online). ΔE (upper) and $M_{\rm bc}$ (lower) distributions for (from left to right) $B^0 \to \eta'\phi$, $B^0 \to \eta'\eta$, $B^0 \to \eta'\eta'$, and $B^0 \to \eta'\omega$.

(2%), uncertainties of the subdecay branching fractions as given by the PDG (1.7%–3.0%), the number of $B\bar{B}$ mesons produced (1.4%), and the uncertainty from particle identification (0.5%–1.3%). In addition, we calculate systematic uncertainties for the fitting procedure by varying all PDF shape parameters by $\pm 1\sigma$. Background normalization systematic uncertainties are estimated by varying the background normalizations by 20%–50% while those for $\Delta E/M_{\rm bc}$ corrections are obtained by varying the corrections by 1 standard deviation. Since for most decays the fits yield branching fractions close to zero, we use absolute errors in these cases. Fractional errors are translated into absolute values by multiplying the obtained upper limit value by the fractional error. The combined absolute errors are decay dependent and lie in the range (0.01–4.93) $\times$ 10^{-6}. The total systematic uncertainties are listed in Table VI.

TABLE VI. Total systematic uncertainties for each decay. Listed are combined errors for fitting, efficiency related errors, and the error in the number of $B\bar{B}$ events. Conservatively, we take the total systematic error to be the linear sum of these. All errors are in absolute values in units of 10^{-7}.

Decay	Fitting	Efficiency	$\#B\bar{B}$	Total
$B^0 \to \eta'\rho^0$	$^{+0.33}_{-1.76}$	0.07	0.02	$^{+0.42}_{-1.85}$
$B^+ \to \eta'\rho^+$	$^{+2.90}_{-5.53}$	0.32	0.06	$^{+3.28}_{-5.91}$
$B^0 \to \eta'K^{*0}$	$^{+0.04}_{-0.03}$	0.16	0.04	$^{+0.24}_{-0.23}$
$B^+ \to \eta'K^{*+}$	$^{+0.84}_{-10.10}$	0.21	0.04	$^{+1.09}_{-10.35}$
$B^0 \to \eta'\phi$	± 0.10	0.03	0.01	± 0.14
$B^0 \to \eta'\eta$	$^{+2.43}_{-0.36}$	0.26	0.05	$^{+2.74}_{-0.67}$
$B^0 \to \eta'\eta'$	$^{+24.85}_{-48.94}$	0.29	0.05	$^{+25.19}_{-49.28}$
$B^0 \to \eta'\omega$	$^{+0.58}_{-5.19}$	0.16	0.03	$^{+0.77}_{-5.38}$

VII. UPPER LIMIT CALCULATION

Since no decay has more than 2σ significance [21], we calculate upper limits on the branching fractions by integrating the likelihood function starting at $\mathcal{B} = 0$ using a Bayesian approach assuming a uniform distribution for $\mathcal{B} > 0$. We set the upper limit when the integral reaches 90% of the total area under the likelihood function. The systematic error is accounted for by folding the systematic error into the width of the likelihood distribution (Eq. (1)) when integrating the likelihood. Thus the upper limit (UL) is calculated with the formula:

$$\frac{\int_{\mathcal{B}=0}^{\rm UL} L_{\rm sys}(N_S, N_{B_j})d\mathcal{B}}{\int_{\mathcal{B}=0}^{1} L_{\rm sys}(N_S, N_{B_j})d\mathcal{B}} = 0.9, \qquad (2)$$

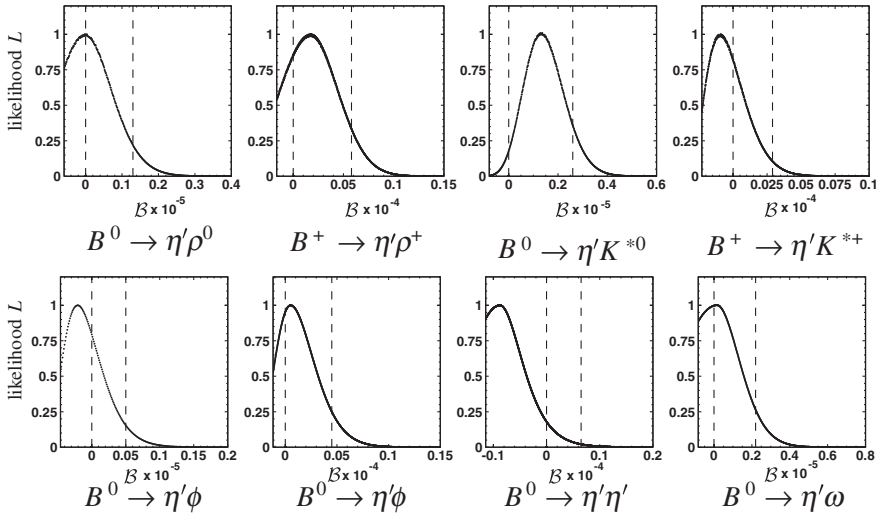

FIG. 3. Distributions of likelihood vs branching fraction for each decay. The systematic error is included as described in the text. Two dashed lines indicate $\mathcal{B} = 0$ and the 90% confidence level upper limit.

where $L_{\rm sys}(N_S, N_{B_j})$ is the likelihood function with its width increased by the systematic error. The likelihood distribution is shown in Fig. 3 for each decay mode.

The thus calculated upper limits are 0.5×10^{-6} for $B^0 \to \eta'\phi$, 1.3×10^{-6} for $B^0 \to \eta'\rho^0$, and in the range 2.2–6.5 $\times 10^{-6}$ for other modes, as given in Tables IV and V. We note that our upper limits for $B^0 \to \eta' K^{*0}$ and $B^+ \to \eta' K^{*+}$ are below the central values of the *BABAR* measurement.

VIII. SUMMARY

In summary, no signal was observed with more than 2σ significance and stringent upper limits in the range $(0.5\text{–}6.5) \times 10^{-6}$ for the decays $B \to \eta'\rho$, $B \to \eta' K^*$, $B^0 \to \eta'\phi$, $B^0 \to \eta'\eta^{(\prime)}$, and $B^0 \to \eta'\omega$ have been given. All limits except $B^0 \to \eta'\eta$ are the most stringent upper limits presently available. Our upper limits for $B \to \eta' K^*$ are below *BABAR*'s central value.

ACKNOWLEDGMENTS

We thank the KEKB group for the excellent operation of the accelerator, the KEK cryogenics group for the efficient operation of the solenoid, and the KEK computer group and the National Institute of Informatics for valuable computing and Super-SINET network support. We acknowledge support from the Ministry of Education, Culture, Sports, Science, and Technology of Japan and the Japan Society for the Promotion of Science; the Australian Research Council and the Australian Department of Education, Science and Training; the National Science Foundation of China and the Knowledge Innovation Program of the Chinese Academy of Sciences under Contract No. 10575109 and No. IHEP-U-503; the Department of Science and Technology of India; the BK21 program of the Ministry of Education of Korea, the CHEP SRC program and Basic Research program (Grant No. R01-2005-000-10089-0) of the Korea Science and Engineering Foundation, and the Pure Basic Research Group program of the Korea Research Foundation; the Polish State Committee for Scientific Research; the Ministry of Science and Technology of the Russian Federation; the Slovenian Research Agency; the Swiss National Science Foundation; the National Science Council and the Ministry of Education of Taiwan; and the U.S. Department of Energy.

[1] B. Aubert *et al.* (*BABAR* Collaboration), Phys. Rev. Lett. **95**, 131803 (2005).
[2] J. Schümann *et al.* (Belle Collaboration), Phys. Rev. Lett. **97**, 061802 (2006).
[3] B. Aubert *et al.* (*BABAR* Collaboration), Phys. Rev. Lett. **98**, 051802 (2007).
[4] C. W. Chiang, M. Gronau, J. L. Rosner, and D. A. Suprun, Phys. Rev. D **70**, 034020 (2004).
[5] M. Beneke and M. Neubert, Nucl. Phys. **B675**, 333 (2003).
[6] H. K. Fu, X. G. He, and Y. K. Hsiao, Phys. Rev. D **69**, 074002 (2004).
[7] B. Aubert *et al.* (*BABAR* Collaboration), Phys. Rev. D **73**, 071102 (2006).
[8] S. Kurokawa and E. Kikutani, Nucl. Instrum. Methods Phys. Res., Sect. A **499**, 1 (2003), and other papers included in this volume.

[9] A. Abashian *et al.* (Belle Collaboration), Nucl. Instrum. Methods Phys. Res., Sect. A **479**, 117 (2002).
[10] Z. Natkaniec *et al.* (Belle SVD2 Group), Nucl. Instrum. Methods Phys. Res., Sect. A **560**, 1 (2006).
[11] F. Fang, Ph.D. thesis, University of Hawaii, 2003.
[12] S. Eidelman *et al.* (Particle Data Group), Phys. Lett. B **592**, 1 (2004).
[13] The Fox-Wolfram moments were introduced in G. C. Fox and S. Wolfram, Phys. Rev. Lett. **41**, 1581 (1978); The Fisher discriminant used by Belle, based on modified Fox-Wolfram moments (SFW), is described in K. Abe *et al.* (Belle Collaboration), Phys. Rev. Lett. **87**, 101801 (2001); Phys. Lett. B **511**, 151 (2001); Here, six of the possible eight Fox-Wolfram moments were used, however, R_1^{OO} was later found to be correlated with $M_{\rm bc}$ for two-body decays and therefore is omitted in this analysis leaving the five SFW moments R_2^{SO}, R_2^{OO}, R_3^{OO}, R_4^{SO}, and R_4^{OO}.
[14] R. A. Fisher, Annals of Eugenics **7**, 179 (1936).
[15] R. Ammar *et al.*, Phys. Rev. Lett. **71**, 674 (1993).
[16] H. Kakuno *et al.*, Nucl. Instrum. Methods Phys. Res., Sect. A **533**, 516 (2004).
[17] D. J. Lange, Nucl. Instrum. Methods Phys. Res., Sect. A **462**, 152 (2001).
[18] E. Barberio and Z. Wąs, Comput. Phys. Commun. **79**, 291 (1994).
[19] J. E. Gaiser *et al.* (Crystal Ball Collaboration), Phys. Rev. D **34**, 711 (1986).
[20] H. Albrecht *et al.* (ARGUS Collaboration), Phys. Lett. B **241**, 278 (1990).
[21] The statistical significance of the signal is calculated as $\sigma = \sqrt{2\ln(L_{\text{max-sys}}/L_0)}$, where L_0 and $L_{\text{max-sys}}$ denote the likelihood value at zero branching fraction and the value at 1 standard deviation of the systematic error below the maximum likelihood, respectively.